Molecular Crystals and Liquid Crystals Science and Technology. Section A. Molecular Crystals and Liquid Crystals

Publication details, including instructions for authors and subscription information:
http://www.tandfonline.com/loi/gmcl19

Anchoring Transitions of Nematic Liquid Crystals in a Lattice Model

J. Chakrabarti [a] & B. M. Mulder [a]

[a] FOM Institute for Atomic and Molecular Physics, PO. Box 41883, 1009 DB, Amsterdam, The Netherlands

Version of record first published: 04 Oct 2006

To cite this article: J. Chakrabarti & B. M. Mulder (1998): Anchoring Transitions of Nematic Liquid Crystals in a Lattice Model, Molecular Crystals and Liquid Crystals Science and Technology. Section A. Molecular Crystals and Liquid Crystals, 323:1, 97-112

To link to this article: http://dx.doi.org/10.1080/10587259808048435

Mol. Cryst. Liq. Cryst., Vol. 323, pp. 97–112
Reprints available directly from the publisher
Photocopying permitted by license only

Anchoring Transitions of Nematic Liquid Crystals in a Lattice Model

J. CHAKRABARTI and B. M. MULDER*

FOM Institute for Atomic and Molecular Physics, P.O. Box 41883, 1009 DB Amsterdam, The Netherlands

(Received 13 May 1997; In final form 1 May 1998)

We investigate the effect of surface ordering on the bulk anchoring and anchoring transition of a nematic liquid crystal placed in the contact with a solid substrate. We model this situation by a simple lattice spin model in a semi-infinite geometry, where we impose the orientational distribution function (ODF) at the planar boundary. Mean field calculations, verified by Monte Carlo calculations, show that the *anchoring transitions* in the system are fully determined by the parameters of the imposed boundary ODF.

Keywords: Nematic; director; anchoring transition; boundary orientation distribution

Mathematical Subject Classification: 61.30. G

1. INTRODUCTION

The orientation of the preferred axis of a homogeneous nematic phase in the absence of external influences, is infinitely degenerate. This degeneracy is the consequence of the fact that the nematic phase arises from the spontaneous breaking of the continuous rotational symmetry of the isotropic phase. One way to lift this degeneracy is to bring a nematic sample into contact with a solid substrate. Due to the interactions with the substrate the director in the bulk of the sample, *i.e.*, far away from the substrate picks up a unique orientation. This effect is known as the *anchoring* of the liquid crystal. The phenomenon of orientation of nematic liquid crystals by surfaces is as well

*Corresponding author. e-mail: mulder@amolf.nl

studied as the liquid crystals themselves for both fundamental reasons and technical (display) applications [1]. The anchoring induced by a solid substrate is particularly interesting, for changes in the bulk anchoring direction, *i.e.*, *anchoring transitions*, can be induced by (small) changes in the conditions right at the substrate [1].

We can distinguish three regions in a nematic liquid crystal in contact with a substrate. Far from the contact surface, we have a bulk nematic liquid crystal with uniform orientation of the director. Right at the surface, the orientation of liquid cyrstal molecules in direct contact with the substrate is strongly determined by their interaction with the substrate. In between there is an interfacial region, through which the nematic order evolves from the surface order to the bulk order. Recent second harmonic generation (SHG) experiments [2] have shown that it is possible to reconstruct in detail the orientational distribution function (ODF) induced right at the solid substrate. There have been a number of recent experiments [2, 3, 7] which elucidate the connection between the ODF at the substrate, determined from SHG experiments and the bulk anchoring transition. Jérôme and Shen [3] study the anchoring of nematic liquid crystalline molecules, like 5OCB and 5CB on cleaved surface of muscovite mica in the presence of volatile ethylene glycol vapour. With increasing ethylene glycol concentration, the peaks of the ODF at the substrate, as probed by SHG experiments, undergo an abrupt change at some critical concentration of the vapour and simultaneously the planar bulk director is observed to undergo azimuthal reorientation namely, from a perpendicular to a parallel orientation with respect to the mirror symmetry plane of the underlying substrate. Recently Schuddeboom and Jérôme [7] have carried out systematic experiments on the anchoring of 5OCB and 7CB in the presence of water vapour on a highly anisotropic substrate, phlogopite mica, which has a three fold symmetry axis. The ODF induced at the substrate, probed by SHG, has a three fold symmetric structure as well, reflecting the symmetry of the underlying substrate. With increasing vapour pressure, the tilt distribution of the three fold symmetric ODF with respect to the substrate normal is observed to change and the planar bulk director reorients in the azimuthal plane at a critical pressure from perpendicular to parallel with respect to one of the substrate symmetry axes.

From a statistical mechanical point of view such systems are highly complicated because of their inherent inhomogeneity close to the boundary, and an adequate modelling of the substrate effect is a challenging task. Conventionally a surface potential is assumed in the free-energy that reflects the symmetry of the substrate. Landau-de Gennes theory based on a poly-

nomial expansion of the free energy in the nematic order parameter, has been successfully applied to understand anchoring transitions [8]. But this type of theory is highly phenomenological in character. The expansion coefficients in general have an unknown dependence on experimental parameters. More microscopic approaches, invariably based on some form of density functional theory, tend to simplify the problem by neglecting the inhomogeneity of the interfacial region, and assuming that the LC behaves bulk-like right up to the surface. However, the SHG experiments [2, 3, 7] suggest that the ODF at the boundary, clearly dominated by strong coupling to the substrate, is not even reminiscent of the distribution in the bulk and hence one cannot neglect the relaxation of surface induced order to the bulk order through the interfacial region. This clearly calls for a microscopic calculation which retains the interfacial region as well. We are thus led to propose an approach where the boundary ODF, determined *e.g.*, by SHG experiments, is directly used as input to theory. The bulk ODF is calculated using microscopic interaction, treating the SHG generated ODF as a boundary condition. This step would allow us to determine how the symmetry of the boundary layer propagates through the interfacial region to yield the asymptotic bulk behaviour. Our main goal is to understand which features of the boundary ODF are responsible for determining the bulk anchoring direction. In this way one can build up an anchoring phase-diagram in terms of parameters that characterize the boundary ODF. We discuss the mean field theory that we apply here in Section 2. First we test our approach on a tutorial example: the simplest model available for a nematic *viz.* the Lebwohl-Lasher (LL) model with a uniaxial and a biaxial boundary ODF, as illustrated in Section 3. Next we take up the case of highly anisotropic boundary distributions, more specifically a three-fold boundary ODF as in Ref.[7], detailed in Section 4. We conclude the paper in Section 5 with some remarks. An Appendix contains the details of the derivation of the mean-field free energy functional employed.

2. MEAN FIELD THEORY

We model the nematic liquid crystal as a system of classical spins on a cubic lattice, where each spin interacts with its nearest neighbours through an interaction $V(\omega, \omega')$, which depends on γ, the angle between two spins with orientations $\omega (\equiv \theta, \phi)$ and ω'. The lattice is infinite in the x and y directions and bounded in the z direction. The whole system can be viewed as a stack of planar surfaces with the z-axis as normal to the planes. The ODF for the

α-th plane is denoted by $\rho^{(\alpha)}(\omega)$. The planar surface at which we fix the substrate induced ODF $\rho^{(0)}(\omega)$ is located at the $z = 0$ boundary. For convenience we introduce a free boundary at $z = N$, taking care that N is large enough so as to allow bulk behaviour to develop. For concreteness we identify the polar axis with respect to which the orientations of the spins are defined, with the z-axis of the lattice, which defines our lab frame. We treat this model within the mean-field approximation. Although, strictly speaking, only valid for the case of weak long-ranged interactions, this approximation is the starting point for most analyses of interfacial phenomena [4], and has been employed in the context of lattice systems as well [5], [6]. In 3D, and sufficiently far from phase boundaries, where fluctuation effects are minor and interfaces generally sharp, the mean-field approach is at least expected to provide a qualitatively correct picture. The mean field free energy per column of spins perpendicular to the boundary is given by the following functional of the set of ODFs $\{\rho^{(\alpha)}(\omega)\}_{\alpha = 1,2,\ldots,N}$

$$F[\rho^{(\alpha)}(\omega)] = k_B T \sum_{\alpha=1}^{N} \int d\omega \rho^{(\alpha)}(\omega) \ln \rho^{(\alpha)}(\omega) \tag{1}$$

$$+ \sum_{\alpha=1}^{N} \int d\omega d\omega' \rho^{(\alpha)}(\omega) V(\omega, \omega') [4\rho^{(\alpha)}(\omega') + \rho^{(\alpha-1)}(\omega') + \rho^{(\alpha+1)}(\omega')] \tag{2}$$

The derivation of the mean-field free energy functional for an inhomogeneous lattice model is discussed in the Appendix. The self-consistency equation for the ODF obtained from Eq. (2) are:

$$\rho^{(\alpha)}(\omega) = \frac{1}{Z^{(\alpha)}} \exp -\beta H^{(\alpha)}(\omega) \tag{3}$$

where

$$H^{(\alpha)}(\omega) = \int d\omega' V(\omega, \omega') [4\rho^{(\alpha)}(\omega') + \rho^{(\alpha-1)}(\omega') + \rho^{(\alpha+1)}(\omega')] \tag{4}$$

and

$$Z^{(\alpha)} = \int d\omega \exp -\beta H^{(\alpha)}(\omega) \tag{5}$$

which taken care of the normalisation of $\rho^{(\alpha)}$.

It is convenient to decompose the ODF in spherical harmonics basis [11], $\rho^{(\alpha)} = \Sigma_l \Sigma_{m=-l,l} \rho_{lm}^{(\alpha)} Y_{lm}$. The ODF at the zeroth layer, $\rho^{(0)}(\omega)$ or equivalently

$\{\rho_{lm}^{(0)}\}$, is taken as a given input and the mean field free energy is minimized in the space of $\{\rho_{lm}^{(\alpha)}\}$. The free boundary far away from the substrate is implemented by setting $\rho^{(N+1)}(\omega) = 1/4\pi$. Once the components of the ODF are calculated, the standard symmetric second rank nematic tensor Q can be constructed:

$$\begin{aligned} Q_{xx} &= \frac{\sqrt{3}}{2} Re\rho_{22}^{(\alpha)} - \frac{1}{2}\rho_{20}^{(\alpha)}, \\ Q_{zz} &= \rho_{20}^{(\alpha)}, \\ Q_{yy} &= -Q_{xx} - Q_{zz}, \\ Q_{xy} &= \frac{1}{2} Im\rho_{22}^{(\alpha)}, \\ Q_{xz} &= Re\rho_{21}^{(\alpha)}, \\ Q_{yz} &= Im\rho_{21}^{(\alpha)}. \end{aligned} \tag{6}$$

The nematic scalar order parameter S is given by the largest eigenvalue of Q and the director is the corresponding eigenvector.

3. TUTORIAL EXAMPLE: LL MODEL

First we consider the simplest available model for Nematic phases, namely the Lebwohl–Lasher (LL) [10] model where the spin–spin interaction $V(\omega, \omega') = -JP_2[\cos(\gamma)]$, where J is the interaction strength, P_2 is the 2nd order Legendre Polynomial, and γ is the angle between two spins. The self-consistency Eq.(3) for density will now read:

$$\rho^{(\alpha)}(\omega) = \frac{1}{Z^{(\alpha)}} \int d\omega' \exp[-JP_2(\hat{\omega}.\hat{\omega}')(4\rho^{(\alpha)}(\omega') + \rho^{(\alpha-1)}(\omega') + \rho^{(\alpha+1)}(\omega'))],$$

where $\hat{\omega}$ is a unit vector in the direction of ω. Decomposing $P_2(\hat{\omega}.\hat{\omega}')$ into products of spherical harmonics, it is easy to see that the components with $l = 2$ are the only relevant ones. We consider as an illustration, a simple conical boundary ODF $\rho^{(0)}(\omega) = \delta(\theta - \Psi)/2\pi \sin\Psi$, characterized by the opening angle Ψ. It is a uniaxial boundary ODF for which $\rho_{20}^{(0)} = P_2(\cos\Psi)$ and $\rho_{22}^{(0)} = 0$. The director at the boundary is parallel to z-axis for any Ψ. A zero temperature calculation shows that the possible ground states have a mirror symmetry plane through the polar axis, degenerate with respect to rotations about the polar axis. Hence $\rho_{20}^{(\alpha)}$ and $\rho_{22}^{(\alpha)}$ are the only relevant modes. We restrict our attention to temperature sufficiently below the bulk

nematic–isotropic transition, which for this model occurs at $k_BT/J = 1.32$. Under these conditions we find that the interfacial region, characterized by variations of the scalar order parameter S is small, typically two layers thick. The director is found to be uniform throughout the system for all layers with $\alpha \geq 1$. For $\Psi < \Psi_{\text{magic}} = 54.7°$ the anchoring direction is homeotropic (parallel to z-axis) while for $\Psi > \Psi_{\text{magic}}$ planar (perpendicular to z-axis) alignment occurs, independent of temperature (Fig. 1). In the planar case the inplane direction of the director is of course degenerate with respect to rotations about the z-axis. The occurrence of an anchoring transition at $\Psi = \Psi_{\text{magic}}$ is easily understood when one realizes that for in this case $\rho_{20}^{(0)} = 0$, so that the liquid crystal effectively decouples from the substrate given the nature of the LL interaction.

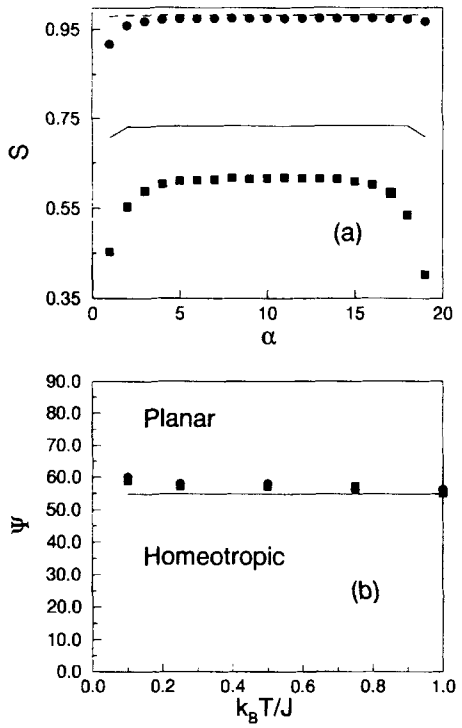

FIGURE 1 LL interaction with a uniaxial boundary ODF: (a) Nematic Scalar order parameter (S) as a function of layer index (α) from mean field calculation (solid line for $k_BT/J = 1.0$ and dashed line for $k_BT/J = 0.1$) with $\rho_{20}^{(0)} = -.125$ and simulation results (filled boxes for $k_BT/J = 1.0$ and filled circles for $k_BT/J = 0.1$) with $\Psi = 60°$. (b) Anchoring transition line (in Ψ *vs* k_BT/J plane) between bulk homeotropic and planar alignments: mean field result (solid line), Monte Carlo for conical boundary distribution (filled squares) and Monte Carlo for 3-fold symmetric boundary distribution (filled circles).

We verify our theoretical predictions by means of Monte Carlo simulations. We use a $20 \times 20 \times 20$ system with periodic boundary conditions in the x and y directions. The boundary ODF is imposed at the $z = 0$ plane, by selecting each boundary spin independently from the intended distribution. These spins are then left fixed throughout the simulation. The rest of the spins are initially taken to be parallel to the z-axis and are updated according to the standard Metropolis algorithm. First, hundred thousand steps are discarded to allow the system to reach equilibrium, except for Ψ close to the magic angle (the mean field anchoring transition line) where the equilibration run is typically twice as long. After equilibration, every ten MC steps, the nematic tensor order parameter is constructed for each layer according to the formula: $Q_{ij} = \sum_\alpha (\frac{3}{2} x_i^\alpha x_j^\alpha - \frac{1}{2}\delta_{ij})$ where α indicates the particles and i, j indicate the Cartesian components. This tensor is diagonalised; the numerically largest eigenvalue is taken to be S and the corresponding eigenvector is the director. S is averaged over ten thousand configurations. We have checked that the reuslts do not depend on the specific realization of the boundary distribution. Our results show that here too the interfacial region is small and that the director is uniform throughout the system. For the director we compute the histograms for the distribution of the polar angles in the lab frame. We find that the histogram for polar angle distribution shows a sharp peak that changes from close to $\theta = 0°$ (homeotropic) to that close to $\theta = 90°$ (planar) for values of Ψ close, albeit systematically above, the magic angle (Fig. 1). This deviation increases as one lowers $k_B T/J$. In order to understand the reason behind the systematic deviation we repeat our simulations for the lowest temperature with an initial planar configuration of the spins, with identical boundary distributions. It turns out that the transition point in this case falls below the theoretical prediction. A zero temperature calculation shows that the energy cost of turning the spins of the first layer at an angle θ while keeping the spins on the zeroth layer at the magic angle and the rest of the spins parallel to z-axis, given by: $-(1/3)(2 + \cos 2\theta)$ apart from constants, increases with θ within the interval $\theta = 0$ to $\pi/2$. This indicates that the planar and the homeotropic configurations are separated by a high free energy barrier which becomes more and more important as $k_B T/J$ is lowered, leading to the observed deviation.

To verify our prediction that the anchoring in this model should depend only on the sign of $\rho_{20}^{(0)}$, we have considered a three-fold symmetric boundary ODF as in Ref. [7] $\rho^{(0)}(\omega) \sim \delta(\theta - \Psi)[\delta(\phi) + \delta(\phi - 2\pi/3) + \delta(\phi - 4\pi/3)]$. Although this boundary ODF is more anisotropic than the conical boundary ODF, only $\rho_{20}^{(0)} \neq 0$ and $\rho_{22}^{(0)} = 0$ exactly as in the conical case.

The results, also plotted in Figure 1 are indeed close to that of the conical case. The difference between the conical and the three-fold boundary ODF shows up only in higher l order parameters, suggesting the requirement of having higher l terms in the spin – spin interaction to understand the anchoring transition of Ref. [7].

Before we take up the case of higher order spin – spin interactions, we consider the relaxation of a biaxial boundary ODF, *i.e.*, $\rho_{22}^{(0)} \neq 0$, to the uniaxial bulk ODF retaining simple LL interactions between the spins. We carry out mean field calculations for a given $\rho_{22}^{(0)}$ and $\rho_{20}^{(0)}$, based on free energy in Eq. (2). The difference between the two smaller eigenvalues of the nematic tensor, Q obtained from Eq. (6), is the measure of biaxiality (δ). We show S and δ as a function of the layer index for a typical case in Figure 2(a). It is clear that the boundary biaxiality decays to zero in the bulk over

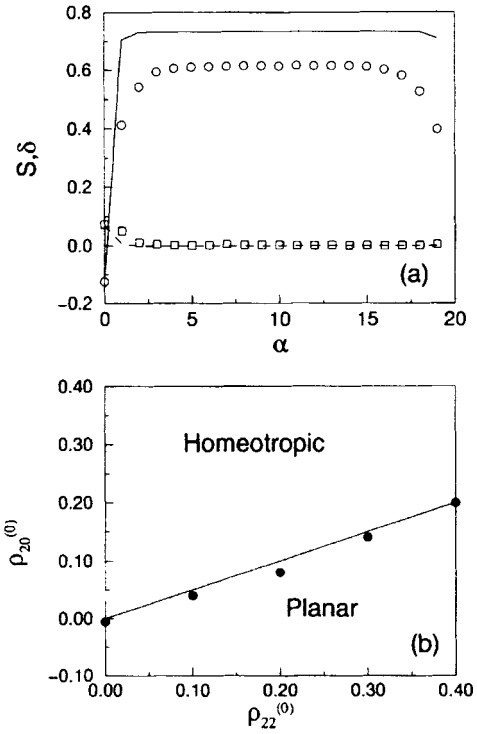

FIGURE 2 LL interaction with a biaxial boundary ODF: (a) Nematic Scalar order parameter (S) (solid line from mean field theory and open circles from simulation) and biaxiality (δ) (dashed line from theory and open boxes from simulation) as a function of layer index (α) for $\rho_{20}^{(0)} = -0.125$, $\rho_{22}^{(0)} = 0.2$ at $k_BT = 1.0$. (b) Anchoring diagram in $\rho_{22}^{(0)}$, $\rho_{20}^{(0)}$ plane for $k_BT = 1.0$ (solid line from theory and the filled circles from simulation).

the tiny interfacial region. The director is uniform throughout the system. The bulk director is homeotropic above $\rho_{20}^{(0)} = \rho_{22}^{(0)}/2$ line and planar below this line, as shown by the solid line in Figure 2(b). The anchoring transition line is independent of k_BT/J as before. This result is simple to understand since the director at the boundary itself becomes planar as one goes below this line. We check the mean field results by means of Monte Carlo simulations. We choose the boundary spins from a distribution $P(\theta, \phi) = C\exp(AP_2(\cos\theta) + B\sin^2\theta\cos 2\phi)$, where C takes care of the normalisation and A, B are such as to satisfy $\int d\omega P_2(\cos\theta)P(\theta,\phi) = \rho_{20}^{(0)}$ and $\int \sin^2\theta\cos\phi P(\theta,\phi) = \rho_{22}^{(0)}$ for the given $\rho_{20}^{(0)}$ and $\rho_{22}^{(0)}$. The transition points as found from the simulation, shown by the filled circles in Figure 2(b), is in clear agreement with our mean field predictions. The agreement between the theoretical and simulation results for this simple model leads us to use our formalism for more complicated cases.

4. ANISOTROPIC BOUNDARY ODF AND MORE COMPLICATED INTERACTION POTENTIALS

Now we generalize the above mean field analysis to the anisotropic boundary ODF, more specifically the three fold symmetric boundary ODF. As already pointed out, we need to include higher order l terms in the spin–spin interaction to address these situations. We note that due to up–down symmetry of the nematic phase only even l are allowed in the spin–spin interaction. If we consider the presence of a $P_4(\cos\gamma)$ term in addition to the usual LL interaction, $\rho_{lm}^{(\alpha)}$ for both $l = 2$ and $l = 4$ will be relevant. In this case in addition to $\rho_{20}^{(0)}$, $\rho_{40}^{(0)}$ and $\rho_{43}^{(0)}$ are also relevant boundary parameters. The presence of these higher order boundary order parameter make the anchoring diagram nontrivial. For instance, the azimuthal symmetry is expected to be broken due to the presence of a nonzero $\rho_{43}^{(0)}$.

We illustrate from our mean field calculations the main features of the bulk anchoring due to the presence of a nonzero $P_4(\cos\gamma)$ term with a three-fold symmetric boundary ODF with mirror symmetry axis (C_{3v}). We choose the lab frame as follows: the polar axis still coincides with z-axis, but x-axis is taken to coincide with one of the mirror symmetry axis (σ) of the boundary distribution, the azimuthal angle ϕ being measured from this axis. We take the straight forward generalization of the mean field free energy of Eq. (2) for $V(\omega,\omega') = \Sigma_{l=2,4} J_l P_l(\cos\gamma)$. We find that the director evolves from a homeotropic alignment to a quasi-planar alignment (with the polar angle of the bulk director θ_{bulk} close to $(\pi/2)$) through tilted alignments as

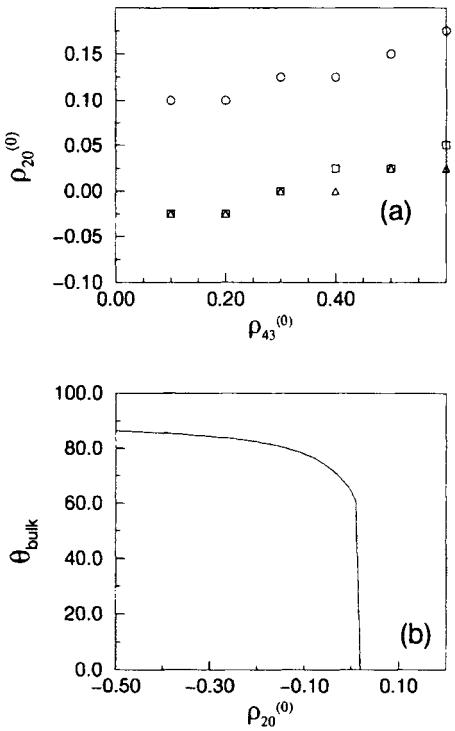

FIGURE 3 (a) The transition line between homeotropic (above the line) and tilted alignments (below the line) for $\rho_{40}^{(0)} = -0.3$ (circles), 0.1 (squares) and 0.3 (triangles) with $P_4(\cos\gamma)$ term in the interaction and a 3-fold boundary ODF. The calculations are done with $J_4/J = 0.2$, $k_BT/J = 1.0$. (b) The polar angle of the bulk director as a function of $\rho_{20}^{(0)}$ at $\rho_{43}^{(0)} = 0.2$ and $\rho_{40}^{(0)} = -0.1$, the other parameters being the same as in (a).

$\rho_{20}^{(0)}$ decreases. The transition lines between the homeotropic and tilted alignments are shown in Figure 3(a). In Figure 3(b) we show θ_{bulk} as a function of $\rho_{20}^{(0)}$ as the bulk director evolves from homeotropic to quasi-planar alignment through tilted orientations. More interestingly, in all these tilted alignments (including the quasi-planar alignments), the bulk director is parallel to σ (*i.e.*, $\phi_{bulk} = 0$). Hence the inclusion of the $P_4(\cos\gamma)$ term in the interaction leads to azimuthal symmetry breaking with a three fold symmetric boundary ODF. However, this does not lead to azimuthal reorientation, observed in Ref. [7].

Next we study the effect of adding biaxiality to the 3-fold symmetric boundary ODF on the anchoring diagram; more interestingly, if it could lead to azimuthal reorientation. As soon as the biaxiality is turned on, or equivalently $\rho_{22}^{(0)} \neq 0$, the three lobes of the boundary ODF become unequal. Let us first consider the case where $\rho_{22}^{(0)}$ is positive. A typical anchoring

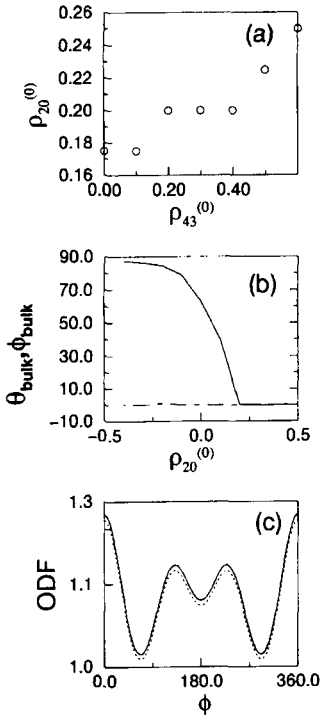

FIGURE 4 (a) Anchoring phase diagram in $\rho_{20}^{(0)}$, $\rho_{43}^{(0)}$ plane with a $P_4(\cos\gamma)$ term in the interaction for $J_4/J = 0.2$, $k_BT/J = 1.0$ and $\rho_{40}^{(0)} = 0.3$ with $\rho_{22}^{(0)} = 0.1$. (b) θ_{bulk} (solid line), ϕ_{bulk} (long dashed line) as functions of $\rho_{20}^{(0)}$ for $\rho_{43}^{(0)} = 0.1$. (c) Azimuthal dependence of boundary ODF for a typical θ with $\rho_{20}^{(0)} = 0.175$ (solid line), 0.15 (dashed line) and -0.3 (dotted line). The difference in the ODF with $\rho_{20}^{(0)}$ is not significant but can cause quite significant chages in the bulk director orientations as can be seen from (b).

diagram in $\rho_{43}^{(0)}$, $\rho_{20}^{(0)}$ plane is shown in Figure 4(a) for $\rho_{22}^{(0)} = 0.1$, $\rho_{40}^{(0)} = 0.3$ and $J_4/J = 0.2$. For a given $\rho_{43}^{(0)}$, we always get homeotropic anchoring for $\rho_{20}^{(0)}$ larger than a threshold positive value. Below this threshold we get tilted orientations of the bulk director. In Figure 4(b) we show θ_{bulk} and ϕ_{bulk} as a function of $\rho_{20}^{(0)}$ for $\rho_{43}^{(0)} = 0.1$. Evidently the bulk director becomes quasi-planar with decreasing $\rho_{20}^{(0)}$ but always $\phi_{bulk} = 0$. To understand what happens at the boundary while the bulk director orientation changes, we plot in Figure 4(c) the azimuthal dependence of the boundary ODF (for θ corresponding to which the ODF has maxima) for three different values of $\rho_{20}^{(0)}$, two close to the point where θ_{bulk} first becomes nonzero and the other when the director is almost planar. Clearly the lobe at $\phi = 0$ is stronger than the other two lobes implying that the director essentially coincides with the dominant lobe in the azimuthal plane. However, the difference between

the distributions is not really so significant, implying that the anchoring direction is incredibly sensitive to very small tuning of the boundary ODF. The anchoring diagram is shown in Figure 5(a) for the same $\rho_{40}^{(0)}$ and J_4/J but a negative $\rho_{20}^{(0)}(=-0.1)$. For large and positive $\rho_{20}^{(0)}$ we always get a homeotropic anchoring (marked by H in Fig. 5(a)). On decreasing $\rho_{20}^{(0)}$, for $0.1 \geq \rho_{43}^{(0)} \geq 0$, we get transition from H to P alignments where the director is planar but oriented perpendicular to σ (P orientation). This transition line is marked by the solid line connecting filled circles in Figure 5(a). The region of this direct transition, however, depends on the value of $\rho_{40}^{(0)}$; for instance, if $\rho_{40}^{(0)} > 0.3$, this region is completely suppressed. For $0.4 > \rho_{43}^{(0)} > 0.1$, we get transition to tilted orientations of the director (T orientation) from H orientations, by decreasing $\rho_{20}^{(0)}$. The transition line is shown by the solid line

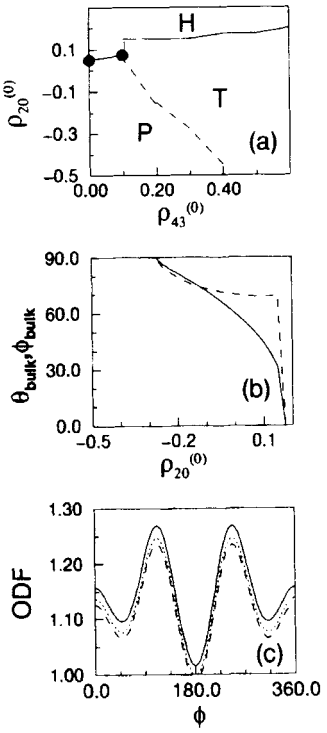

FIGURE 5 (a) Anchoring phase diagram for $J_4/J=0.2$, $k_BT/J=1.0$ and $\rho_{40}^{(0)}=0.3$ with $\rho_{22}^{(0)}=-0.1$. (b) θ_{bulk}(solid line) and ϕ_{bulk}(dashed line) of the bulk director as a function of $\rho_{20}^{(0)}$ for $\rho_{43}^{(0)}=0.3$. (c) Azimuthal dependence of boundary ODF for a typical θ for $\rho_{40}^{(0)}=0.3$, $\rho_{43}^{(0)}=0.2$, $\rho_{20}^{(0)}=1.0$ (solid line), 0.05 (dotted line) and -0.5 (dashed line) with $\rho_{22}^{(0)}=-0.1$. These points correspond to H, T and P orientations respectively in the anchoring diagram in (a).

in Figure 5(a). Further reduction of $\rho_{20}^{(0)}$ in this region of $\rho_{43}^{(0)}$, leads to the transition from T orientation to P orientation, the transition line being shown by the dashed line (Fig. 5(a)). On the other hand if $\rho_{43}^{(0)} > 0.4$, we always get T orientations; the director becomes quasi-planar for large but negative $\rho_{20}^{(0)}$. The most interesting feature for a negative $\rho_{22}^{(0)}$ is the azimuthal reorientation of the bulk director as noted in Figure 5(b). For a negative $\rho_{22}^{(0)}$, the dominant lobe is close to $(2\pi/3)$ (the other equally dominant lobe is related to this lobe by a 3-fold rotation) as shown in Figure 5(c). Unlike the tilted orientations obtained with positive $\rho_{22}^{(0)}$, clearly the bulk director in T orientation makes a finite azimuthal angle with this lobe and both θ_{bulk} and ϕ_{bulk} evolve as a function of $\rho_{20}^{(0)}$. Hence, if the interaction potential is truncated at $P_4(\cos\gamma)$, any interesting azimuthal reorientation of the bulk director can be achieved only through biaxial deformations of the 3-fold boundary ODF which is the case in Ref. [3].

In order to search for the possibility of azimuthal reorientation of the bulk director by tuning the parameters of a purely three-fold symmetric boundary ODF as in Ref. [7], we include a $P_6(\cos\gamma)$ term in the interaction. Note that in this case ρ_{66} will be another relevant order parameter which is nonzero at the boundary by virtue of the 3-fold symmetric ODF and can

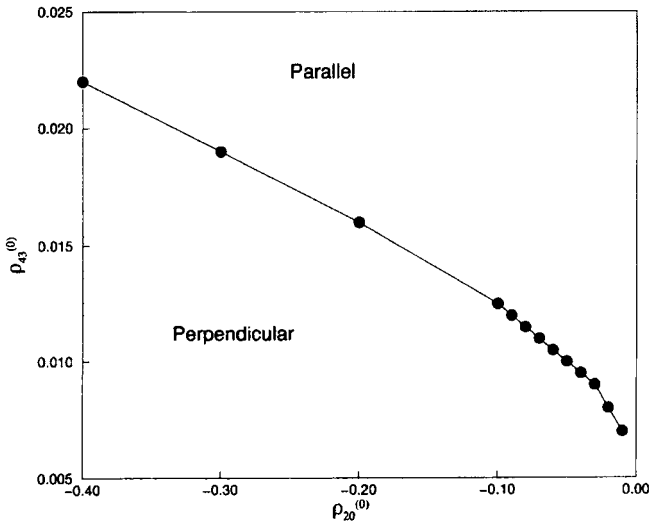

FIGURE 6 The mean field anchoring transition line between (solid line connecting the circles) planar bulk director oriented parallel and perpendicular to mirror symmetry axis (σ) of a three fold symmetric boundary ODF with a $P_6(\cos\gamma)$ term in the interaction and a 3-fold symmetric boundary ODF. The values for different parameters at which the calculations are done: $J_6/J=0.01$, $J_4/J=0.1$, $k_BT/J=1.0$, $\rho_{60}^{(0)}=0.01$, $\rho_{63}^{(0)}=-0.01$, $\rho_{66}^{(0)}=-0.01$ and $\rho_{40}^{(0)}=0.40$.

show spontaneous symmetry breaking for a planar bulk director. This can lead to azimuthal reorientation for a planar bulk director. We carry out mean field calculations ignoring the dependence of $\rho_{20}^{(\alpha)}$ on α. We choose $k_BT/J = 1.0$, $J_4/J = 0.1$ and $J_6/J = 0.01$ and fix $\rho_{40}^{(0)} = 0.4$, $\rho_{60}^{(0)} = 0.1$, $\rho_{63}^{(0)} = 0.1$ and $\rho_{66}^{(0)} = -0.1$. The most interesting observation is that for low values $\rho_{43}^{(0)}$, *i.e.*, for weak anisotropies, we get a planar director with both parallel and perpendicular orientations with respect to σ so far as $\rho_{20}^{(0)} < 0$. The transition line between these two alignments in $\rho_{20}^{(0)}$, $\rho_{43}^{(0)}$ plane, marked by a thick line connecting filled circles in Figure 6, clearly brings out the interesting suggestion that for sufficiently weak anisotropy, by tuning $\rho_{20}^{(0)}$ alone, it is possible to reorient a planar bulk director even in the case of a 3-fold symmetric boundary ODF.

5. CONCLUSION

We have shown that in the context of simple lattice models the link between parameters of the boundary ODF and anchoring behaviour can be fully elucidated. This model calculation shows one possible way to use the SHG data directly in a microscopic calculation to predict the bulk anchoring behaviour. We also stress that this is a microscopic calculation that includes the inhomogeneous interfacial region as well. Our calculation, clearly, can account for azimuthal reorientation of the bulk director induced by highly anisotropic substrates [3, 7]. Our (lattice) model is probably too simple to be compared with experimental results [7]. Nonetheless, it illustrates one possible model compatible with nematic symmetry leading to azimuthal reorientations of the planar director. The basic symmetry considerations will remain valid in more general cases of interactions, namely those which couple the orientational and positional degrees of freedom. However, in order for our approach to have predictive value for real liquid crystals, we need to consider such couplings. It is worthwhile in this context to mention that in order to explain their observed azimuthal reorientation, Schuddeboom and Jérôme [7] in their phenomenological Landau-de Gennes analysis, invoke the coupling between the nematic scalar order parameter and a third rank tensor, which in nonzero due to the three fold pattern at the substrate but decays sufficiently fast in the bulk. They seem to have very good agreement with their experimental numbers [7]. Clearly such couplings are completely ruled out in our analysis, for this corresponds to odd l terms in the spin-spin interaction. It will be interesting to investigate under what situations such coupling can be generated in the light of our microscopic

analysis and compare that with our present microscopic model. We hope to report such comparative studies in a future publication.

Acknowledgements

We thank D. Frenkel, B. Jérôme, P. I. C. Teixeira, R. Blaak and P. Schuddeboom for helpful discussions; B. Jérôme and R. P. Sear for critically reading the manuscript.

References

[1] B. Jérôme, *Rep. Prog. Phys.*, **54**, 391 (1991) and references therein; A. A. Sonin, A. Yethiraj, J. Becchoefer and B. J. Frisken, *Phys. Rev. E.*, **52**, 6260 (1995); D.-F. Gu, S. Uran and C. Rosenblatt, *Liq. Cryst.*, **19**, 427 (1995); P. Hubert, H. Dreyfus, D. Guillon and Y. Galerne, *J. Phys. II*, **5**, 1371 (1995); G. P. Crawford, R. J. Ondris-Crawford, J. W. Doane and S. Zumer, *Phys. Rev. E*, **53**, 3647 (1996).
[2] Y. R. Shen, *Nature*, **337**, 519 (1989); W. Chen, M. B. Feller and Y. R. Shen, *Phys. Rev. Lett.*, **63**, 2665 (1989); G. Marowski, G. Lupke, R. Steinhoff, L. F. Chi and D. Mobius, *Phys. Rev. B*, **41**, 4480 (1990).
[3] B. Jérôme and Y. R. Shen, *Phys. Rev. E*, **48**, 4556 (1993).
[4] See *e.g.*: C. A. Croxton (Editor), Fluid Interfacial Phenomena, John Wiley & Sons (1986).
[5] R. Pandit and M. Wortis, *Phys. Rev. B*, **25**, 3226, (1981).
[6] A. Maritan, G. Langie and J. O. Indekeu, *Physica A*, **170**, 326, (1991).
[7] P. Schuddeboom and B. Jérôme, (to be published).
[8] P. G. De Gennes, *Mol. Cryst. Liq. Cryst.*, **12**, 193 (1971); A. K. Sen and D. E. Sullivan, *Phys. Rev. A*, **35**, 1391 (1987); P. I. C. Teixeira, T. J. Sluckin and D. E. Sullivan, *Liq. Cryst.*, **14**, 1243 (1993); *ibid*, **15**, 939 (1993); A. Di Garbo and M. Nobili, *Liq. Cryst.*, **19**, 269 (1995); A. Poniewierski and A. Samborski, *Phys. Rev. E*, **53**, 2436 (1996).
[9] P. I. C. Teixeira and T. J. Sluckin, *J. Chem. Phys.*, **97**, 1498 (1992); *ibid*, **97**, 1510 (1992); also in P. I. C. Teixeira, *Ph. D. Thesis*, University of Southampton (1993), (Unpublished).
[10] P. A. Lebwohl and G. Lasher, *Phys. Rev. A*, **6**, 426 (1972).
[11] Note that in general the spherical harmonic components ρ_{lm} are complex. We use "*Re*" to refer to the real part of any quantity and "*Im*" to refer to the imaginary part.
[12] H. B. Callen, Thermodynamics and an introduction to Themostatistics, second edition, John Wiley & Sons, New York (1985).

APPENDIX A: THE MEAN-FIELD FREE ENERGY FUNCTIONAL

In this appendix we derive the mean-field free energy for a Lebwohl – Lasher model on a cubic lattice of N layers of M spins, which is inhomogeneous in a single direction. Starting point is the Bogolyubov inequality [12]. Given a system described by hamiltonian $\mathcal{H}$ and an arbitrary reference system described by hamiltonian $\mathcal{H}_0$, then the free energy of the system fulfills the following inequality

$$F \leq \langle \mathcal{H} \rangle_0 - TS_0 \qquad (A1)$$

where the angular brackets denote averaging over the equilibrium ensemble of the reference system and S_0 is the entropy of the reference system. As our reference system we choose a system of non-interacting spins placed in an external field whose strength only depends on the distance to the planar boundary in our semi-infinite geometry, *i.e.*,

$$\mathcal{H}_0 = \sum_{\alpha=0}^{N} \sum_{j=1}^{M} u_\alpha(\omega_{\alpha j}) \tag{A2}$$

where α indexes the parallel planes and j indexes the individual spins within each plane.

The equilibrium distribution of the reference system is given by

$$P_0(\{\omega_{\alpha j}\}) = \prod_{\alpha=0}^{N} \prod_{j=1}^{M} \rho_\alpha(\omega_{\alpha j}) \tag{A3}$$

where the single spin probability is given by

$$\rho_\alpha(\omega) = \frac{e^{-\beta u_\alpha(\omega)}}{\int d\omega' e^{-\beta u_\alpha(\omega')}} \tag{A4}$$

The reference system entropy is easily determined from the definition

$$S_0 = -k_B \int \{d\omega_{\alpha j}\} P_0(\{\omega_{\alpha j}\}) \ln P_0(\{\omega_{\alpha j}\}) = -Mk_B \sum_{\alpha=0}^{N} \int d\omega \rho_\alpha(\omega) \ln \rho_\alpha(\omega) \tag{A5}$$

The system hamiltonian itself is a sum of nearest neighbour interactions

$$\mathcal{H} = \sum_{\langle \mathbf{i},\mathbf{j} \rangle} V(\omega_\mathbf{i}, \omega_\mathbf{j})$$

so that its average over the reference ensemble works out as

$$\langle \mathcal{H} \rangle_0 = M \sum_{\alpha=1}^{N} \iint d\omega d\omega' V(\omega, \omega') \rho_\alpha(\omega) [\rho_{\alpha-1}(\omega') + 4\rho_\alpha(\omega') + \rho_{\alpha+1}(\omega')] \tag{A6}$$

Note that we assume the absence of interactions within the boundary plane. Combining Eqs. (A6) and (A5) yields the free energy per column of spins perpendicular to the boundary as encountered in the main text.